Whole genome sequencing of a family with autosomal dominant features within the oculoauriculovertebral spectrum

Petrin, AL[1]; Machado-Paula, LAM[1]; Hinkle, A[1]; Hovey, L[1]; Awotoye, W[1]; Chimenti, M[2]; Darbro, B[2]; Ribeiro-Bicudo, LA[3]; Dabdoub, SM[1]; Peter, T[1]; Murray, J[2]; Van Otterloo, E[1]; Rengasamy Venugopalan, S[4]; Moreno-Uribe, LM[1]

1 –College of Dentistry and Dental Clinics, University of Iowa, Iowa City, IA, USA
2 – Carver College of Medicine, University of Iowa, Iowa City, IA, USA
3 – Universidade Federal de Goias, Goiania, GO, Brazil
4 - Tufts University School of Dental Medicine, Boston, MA, USA

Corresponding author: Aline L Petrin, Department of Orthodontics, Iowa Institute of Oral Health Research, College of Dentistry and Dental Clinics, University of Iowa, Iowa City, IA, USA. Email: aline-petrin@uiowa.edu

Abstract

Background: Oculoauriculovertebral Spectrum (OAVS) encompasses a wide variety of anomalies on derivatives from the first and second pharyngeal arches including macrostomia, hemifacial microsomia, micrognathia, preauricular tags, ocular and vertebral anomalies. We present the genetic findings of a large three-generation family with multiple members affected with macrostomia, preauricular tags and uni- or bilateral ptosis following an autosomal dominant segregation pattern. **Methods:** We generated whole genome sequencing data for the proband, affected parent and unaffected paternal grandparent followed by Sanger sequencing on 23 family members for the top 10 candidate genes: *KCND2, PDGFRA, CASP9, NCOA3, WNT10A, SIX1, MTF1, KDR/VEGFR2, LRRK1,* and *TRIM2*. We performed parent and sibling-based transmission disequilibrium tests and burden analysis to explore segregation and burden of candidate gene mutations. Bioinformatic analyses investigated the biological connection between genes and the abnormal phenotypes. **Results:** Overall**,** rare missense mutations in *SIX1, KDR/VEGFR2,* and *PDGFRA* showed the best evidence of segregation with the OAV phenotypes in this family. When considering affection with any of the 3 OAVS phenotypes as an outcome, parent-TDTs and sib-TDTs (unadjusted p-values) found that *SIX1* (p=0.025, p=0.052), followed by *PDGFRA* (p=0.180, p=0.069) and *KDR/VEGFR2* (p=0.180, p=0.069) have the strongest associations in this family. Burden analysis via a penalized linear mixed model identified *SIX1* (RC=0.87) and *PDGFRA* (RC=0.98) as having the strongest association with OAVS severity. Using phenotype-specific ogfrautcomes, sib-TDTs identified associations between (1) *SIX1* with uni- or bilateral ptosis (p=0.049) and ear tags (p=0.01), (2) *PDGFRA* and *KDR/VEGFR2* with ear tags (both p<0.01). **Conclusion:** Our study reports the genomic findings of a large family with multiple individuals affected with OAVS phenotypes with autosomal dominant inheritance. Our findings narrow down to three potential candidate genes, *SIX1*, *PDGFRA*, and *KDR/VEGFR2*. Among these, *SIX1* has been previously associated with OAVS ear malformations and it is co-expressed with *EYA1* during ear development. Attempts to strengthen the genotype-phenotype co-relation underlying the OAVS of phenotypes are essential to discover the etiological factors leading to this complex and burdensome condition as well as for family counseling and prevention efforts.

Keywords: macrostomia, preauricular tag, uni- or bilateral ptosis, oculoauriculovertebral, branchial arches, OAVS, whole genome sequencing.

Introduction

Oculoauriculovertebral Spectrum (OAVS) encompasses a wide variety of anomalies on structures derived from the first and second pharyngeal arches, including macrostomia, hemifacial microsomia, micrognathia, preauricular tags, ocular and vertebral anomalies [1]. Although the specific etiology of OAVS anomalies is still elusive the literature describes 3 pathogenic and possibly interacting models that may in part explain craniofacial anomalies, yet not the postcranial findings also described including lung, heart, kidney, skeletal and gastrointestinal anomalies[2]. The pathological models include vascular abnormalities and hemorrhage, abnormal development of cranial neuro crest cells (CNCCs) affecting their migration, proliferation or differentiation and damage to Meckel's cartilage [3]. Healthy dynamics of CNCCs and tissue derivatives within the pharyngeal arches are key during the fourth and eight weeks of embryonic development, a critical stage in human facial formation. During the 5th week, the growing stomodeum is surrounded by multiple, pertinent areas of differentiating cells like the mandibular and maxillary processes, and median and lateral nasal processes that grow, fuse, and differentiate giving rise to the maxillomandibular complex[4].

One of the common findings within the OAVS is macrostomia (Tessier cleft type 7) which accounts for 0.3-1% of facial clefts and is found in about 16-36% of cases with other OAV features [5]. Macrostomia occurs due to the failure in fusion of the maxillary and mandibular processes during week 6th of development. The orotragal line, an embryological line extending from the lateral commissure of the stomodeum to the tragus of the ear, is meant to dissipate once the maxillary and mandibular processes fuse. If fusion fails, then the line continues to develop into the abnormal enlargement of the labial commissure [4]. Anatomically, the abnormal contour of the mouth commissure varies from a mild lateral displacement to a complete transverse cleft to the ear. The orbicularis oris muscle abnormally terminates at this commissure, causing less distance between its location and the tragus [4, 6]. Macrostomia has an incidence of 1 in 60,000 to 1 in 300,000 live births, with more common occurrence in males [7, 8]. While it may occur unilaterally or bilaterally, unilateral cases are more frequent with the right side more often affected than the left side [9].

Although less frequently, the presence of uni- or bilateral ptosis or drooping of the upper eyelid has also been reported in cases within the OAVS [10, 11]. The phenotype can be due defects in the innervation of levator palpebrase superioris muscle, which starts to develop during the fifth week of gestation. It has also been suggested that the OAVS may include defects of the otic placode [1]. The phenotypic complexity of the OAVS, with the involvement of multisystem anomalies suggests that more than one etiological variant is at play.

While the embryological development of the OAVS abnormalities is well understood, the etiology of the defects is not. Environmental factors such as exposure to toxic substances during pregnancy [12, 13], maternal diabetes, and hemorrhage [14] have been associated with OAVS, as well as epigenetic dysregulations [15].

As for the genetic component of OAVS complex etiology, with the advances of next generation sequencing, several genes have been associated however, their pathophysiology remains underexplored. The first gene to be associated with OAVS was *MYT1* [16-19]; after which several others studies reported additional genes, *SF3B2* [20], *ZYG11B* [21], *EYA3* [22, 23], *VWA1* [24], *ZIC3* [25], *AMIGO2* [26], *OTX2*, *YPEL1* [27], *PTCH2* [28]. Structural variants in 4p16, 14q22.3, and 22q11.2 among other loci have also been described [29-38]. Although most causal mutations and structural variants in these genes/loci occur *de novo,* familial inheritance has also been reported, mostly with autosomal dominant inheritance [20, 23, 39-41].

In 2006, researchers Richieri-Costa et. al. investigated a three-generational family with multiple members experiencing macrostomia, preauricular tags, uni- or bilateral ptosis, and external ophthalmoplegia [1]. We report the molecular findings using DNA samples from some affected and unaffected family members. First, we generated whole genome sequencing (WGS)

data for the affected proband, the affected parent, and the unaffected paternal grandparent. Then we followed with Sanger sequencing to investigate segregation of the best candidate genes in the additional available family members.

The objective of this study was to determine the gene(s) that harbor the pathogenic variant that led to the OAVS of abnormalities in the family. These findings support the role of a complex gene network behind craniofacial development and provide additional information for understanding and strengthening of the genotype-phenotype correlations underlying the phenotypic variability present in cases with OAVS.

Methods

Patients

The detailed clinical description of the family was previously published by Richieri-Costa et al (2006) [1]. Briefly, the female proposita presented at birth with bilateral macrostomia, preauricular sinus, and preauricular tags. The parent presented with normal mouth contour and preauricular tags. Other members of the family present one or more of the following: macrostomia, preauricular skin tags, and/or uni- or bilateral ptosis[*]. As previously reported by Richieri-Costa et al (2006) [1], the examined family members had no apparent neurological symptoms, abnormal ocular movement, bulbar signs, limb anomalies, or muscle weakness in the extremities at the time of examination [1]. We obtained DNA samples from 8 affected and 15 unaffected family members across the three generations. The study was approved by the respective institutional review boards and all participants signed informed consents prior collection of clinical data and biological samples.

Whole Genome Sequencing and Variant Calling

We generated whole-genome sequencing (WGS) data (30X coverage) for the proband, affected parent and unaffected paternal grandparent and analyzed the entire genome of the three individuals for pathogenic protein-altering genetic variants that were shared between the proband and the parent but not carried by the unaffected grandparent. Pathogenic variants that segregated within the affected individuals (proband and parent) but not in control (grandparent) were further investigated within the expanded family.

Genomic Analysis workflow: The genomes of the three selected individuals were sequenced at an average coverage depth of 30x. The sequence data were mapped and aligned to the human genome assembly GRCh38 (Hg38). Following the alignment, alternate alleles at each genomic locus were called using the highly performing Dynamic Read Analysis for GENomics (DRAGEN) pipeline [42, 43]. These alternate alleles included single nucleotide variants (SNVs), insertions and deletions (InDels). As a quality control measures, we selected variants with a genotype quality (GQ) of at least 20 and a read depth (RD) of at least 10. Next, we prioritized rare protein-altering genetic variants. These rare variants were selected based on [†]minor allele frequency (MAF) less than 1% (0.01) reported on the genomic population database, gnomAD (https://gnomad.broadinstitute.org/). This pipeline is based on the hypothesis that this familial craniofacial condition is caused by rare protein-altering genetic variant(s). Next, we used the Mouse Genomics Informatics (MGI) Database (https://www.informatics.jax.org) to investigate the association between the genes harboring identified pathogenic variants and craniofacial phenotypes observed in mice prioritizing those similar to the reported traits within the family. We included all variants with gnomAD constraint

[*] The full pedigree is not included in this preprint to protect confidentiality of the patients. For additional information, please contact the corresponding author.

scores less than 0.9 and z scores greater than 3.5 for LOF and missense, respectively, and also included genes with significant craniofacial phenotype in the MGI database.

Next, we used *in silico* tools including Sorting Intolerant From Tolerant, SIFT (http://sift.jcvi.org/), Polymorphism Phenotyping, PolyPhen2[44] (http://genetics.bwh.harvard.edu/pph2/), Combined Annotation Dependent Depletion – CADD score[45] - (https://cadd.gs.washington.edu/) and Varsome[46] – (https://varsome.com/) to predict the pathogenicity of the selected protein-altering variants. In addition, we used the web-based machine-learning algorithm, DOMINO (https://domino.iob.ch/) to assess the probability that the genes harboring these variants are likely to cause dominant changes, thus matching the inheritance pattern of the craniofacial condition in the family.

Sanger Sequencing

We designed primers for mutations located in the top 10 candidate genes (*KCND2, PDGFRA, CASP9, NCOA3, WNT10A, SIX1, MTF1, KDR/VEGFR2, LRRK1,* and *TRIM2)* that resulted from the pipeline described above and sequenced DNA from 23 available family members (affected and unaffected individuals) to investigate the segregation of each mutation. Primer sequences and PCR conditions are available upon request. PCR products were verified in agarose gel and submitted for Sanger sequencing at the University of Iowa DNA Core facility.

Statistical Analysis

After confirming the presence or absence of the mutations in the 23 individuals, we performed three analyses: (1) parent and sibling-based transmission disequilibrium tests (TDTs) to examine associations with any OAVS anomaly, (2) a burden analysis to explore the effects of the candidate gene mutations on OAVS phenotype severity, and (3) parent and sibling-based TDTs to detect associations with specific OAVS phenotypes.

For our first analysis, we classified each individual as being 'affected' or 'unaffected' based on the presence/absence of OAVS abnormalities. Individuals with any one of or any combination of macrostomia, uni- or bilateral ptosis, or ear tags were designated as 'affected.' One of the 23 individuals had an indeterminate phenotype and was believed to be a non-penetrant obligated carrier based on the genotype and family data. The present analysis designated this individual of indeterminate phenotype as 'unaffected,' keeping consistent with previous publications based on this data set. Two statistical tests were performed: the parent-TDT [47] and the sib-TDT [48], both of which are variations of the well-known transmission disequilibrium test (TDT). The parent-TDT combines the traditional TDT with a parental discordance test, thereby treating each nuclear family parental couple as a matched pair in addition to analyzing parent-child trios. The sib-TDT combines the traditional TDT with a sibling-based method, so that unaffected siblings can serve as controls for their affected siblings when genotype data from parents is unavailable. A total of 18 tests of association were implemented using PLINK software (version 1.9).

In the second analysis (burden test), we defined a numeric outcome indicating the number of OAVS anomalies present on an individual. This value ranged from 0 to 3, with 0 representing individuals with no OAVS anomalies and 3 representing individuals with a maximum number of 3 anomalies and therefore greater phenotypic severity. With this outcome, we used a penalized linear mixed modelling (PLMM) approach [49] to identify the genes with the strongest evidence of association with the severity of OAVS phenotypes. This PLMM approach incorporated all the individuals in the data, accounting for the relatedness among family members using the average percentage of DNA shared between relatives (23andMe, 2022). PLMM does not perform association tests for each gene; instead, this method treats the candidate gene mutations as one system and then chooses the members of the system which have the most evidence of association with the severity of the phenotype. PLMM was implemented in R (version 4.3).

For the third analysis, we used parent and sibling based TDTs to generate hypotheses about associations between individual candidate gene mutations and specific OAVS phenotypes. This involved a total of 27 tests, one for each combination of gene and OAVS phenotype.

Since the goals across all three of our analyses were exploratory, no p-values were adjusted for multiple comparisons.

Bioinformatic Analysis

The InterPro database was used to investigate the specific candidate proteins, their domains, and functional sites [50]. For prediction of the potential pathogenic potential of 3D protein structure alterations due to mutations, we used AlphaMissense [51]. Finally, we used MobiDB to investigate protein disorder and mobility annotations [52]. Active subnetwork pathway enrichment analysis of genes determined to be significantly associated (see previous section) was carried out using the R package pathfindR v2.2.0 [53]. Briefly, the list of genes and p-values was loaded as input, genes were filtered through the Biogrid protein interaction network [54, 55] and the resulting set of interactions (with at most one indirect interaction) were used for pathway enrichment analysis through the GO [56] and Reactome [57] databases.

Results

Whole genome Sequencing

To identify novel or rare protein-altering variants, we extracted high confidence LoF (stop-gained, frameshift, and splice acceptor/donor) and missense variants with minor allele frequency ≤1% when compared with the human global and ethnic -specific database (gnomAD) [58]. Following our data analysis pipeline, we identified 14 loss of function (LOF) and 222 missense mutations (Supplemental Table 1) that were present in both the parent and proband but not present in the unaffected grandparent as illustrated in Figure 2.

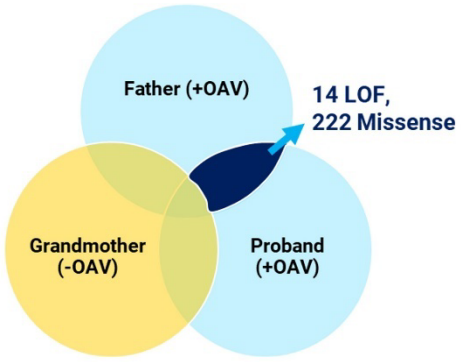

Figure 2: 14 LOF and 222 Missense genes were shared solely between the father (+OAV) and proband (+OAV)

From those, we kept variants with gnomAD constraint scores less than 0.9 and z score greater than 3.5 for LOF and missense (3 genes in Table 1), respectively; and included genes with significant craniofacial phenotype in the MGI database (13 genes in Table 2).

Table 1: Resulting genes based on gnomAD constraint metrics

Gene of Interest	Chr. Pos (hg38)	Effect	Missense Z	pLOF o/e
KCND2	7:120733051	LoF	4.65	0.43
UNC80	2:209819105	Missense	4.99	0.48
TRIM2	4:153257397	Missense	3.94	0.4

Table 2: Resulting genes associated with human and/or mouse craniofacial phenotype based on the Mouse Genomics Informatics Database				
Gene	**Chr. Pos. (hg38)**	**Mutation Effect**	**Human Phenotypes**	**Mouse Phenotypes**
KIAA0586	14:58470656	Missense	Cleft palate, Depressed Nasal Bridge	Abnormal lateral/medial nasal prominence, narrow head
NCOA3	20:47651093	Missense	NA	Abnormal tooth morphology, lower ear position
CASP9	1:15518262	Missense	Hyposmia	Abnormal olfactory epithelium
PDGFRA	4:54288865	Missense	NA	Cleft palate, impaired ossification of basisphenoid bone, decreased cranium height, abnormal frontal/parietal/nasal bone morphology, absent zygomatic bone, ectopic cranial bone, abnormal frontonasal prominence, abnormal nasal capsule, short snout, midline facial cleft
WNT10A	2:218890256	Missense	Shopf-Shulz-Passarge Syndrome, tooth agenesis	Abnormal alveolar process/incisor/molar morphology, dental pulp stones, taurodontia, abnormal dentin morphology, abnormal tooth resorption, abnormal tongue morphology
FER	5:108954852	Missense	NA	Abnormal snout morphology
KDR/VEGFR2	4:55104697	Missense	NA	Abnormal mandibular prominence morphology, absent third/fourth pharyngeal arch, abnormal second pharyngeal arch
SIX1	14:60646457	Missense	Preauricular Pit	Abnormal craniofacial morph, abnormal craniofacial bone morph, abnormal styloid process/Meckel's cartilage/frontal bone morph, short temporal bone squamous part, abnormal hyoid bone greater horn morphology, short mandible, short maxilla, micrognathia, abnormal nasal bone morph, absent turbinates, short zygomatic bone, abnormal incus/malleus/stapes morph, absent stapes, abnormal face development, abnormal midface morph, abnormal genioglossus muscle, dec tongue size, abnormal nose morph, abnormal external nares morph, abnormal nasal cavity morph, absent vomeronasal organ, abnormal/absent olfactory epithelium
KDF1	1:26951399	Missense	Short philtrum (H), natal tooth (H), concave nasal ridge (H)	NA
MTF1	1:37857470	Missense	NA	Palatal shelf fusion with tongue, cleft palate, abnormal tongue epithelium morphology, oral atresia, abnormal nose morphology, short snout
NPHP3	3:132708187	Missense	Meckel syndrome, renal hepatic pancreatic dysplasia, large fontanelles, dandy walker malformation, potter facies, preauricular pit, high forehead	Premature tooth eruption, malocclusion
DUOX2	15:45105795	Missense	NA	Abnormal cranium morphology, abnormal zygomatic bone morphology, abnormal snout morphology
LRRK1	15:101010802	Missense	NA	Abnormal tooth morphology, absent teeth, abnormal mandible morphology, abnormal maxilla morph, abnormal zygomatic morph, abnormal facial morph, abnormal snout morph

Lastly, based on the autosomal dominant inheritance in this family, we used the Domino Database to assess inheritance patterns of the 16 genes that resulted from the filtering steps above. Any genes that had extremely low odds of harboring an autosomal dominant mutation were excluded from candidacy. Only “Likely dominant” to “Very likely dominant” were considered as candidates to harbor etiological variants, which narrowed our list of candidates down to 10 genes (Table 3).

Table 3: Genes with very likely or likely dominant inherited based on Domino Database

Gene of Interest	**Mutation**	**LDA Score**	**P(AD)**	**Class**
SIX1	D227E	3.698	1	Very likely dominant
KCND2	R422*	3.172	1	Very likely dominant
PDGFRA	R914Q	2.857	0.999	Very likely dominant
MTF1	D63E	2.47	0.997	Very likely dominant
KDR/VEGFR2	Q645E	2.336	0.996	Very likely dominant
NCOA3	Q1276del	2.235	0.994	Very likely dominant
LRRK1	L416M	1.104	0.833	Very likely dominant
CASP9	L89P	0.836	0.718	Likely dominant
WNT10A	D217N	0.655	0.624	Likely dominant
TRIM2	12941G>A	0.642	0.617	Likely dominant

P(AD) - Probabilities of being dominant

Segregation Analysis of top 10 candidate genes

Mutations found in the 10 candidate genes that resulted in a likely dominant or very likely dominant were then tested for segregation in additional family members We designed primers specific for each mutation and used Sanger sequencing to confirm presence or absence of the mutations in all available family members. Table 4 below displays the affected and unaffected available family members, their phenotypes, and genotypes for each of the 10 variants analyzed.

Table 4: Genotypes of the top 10 candidate genes in affected and unaffected family members

Degree of relationship to proband	**Phenotype**	***KCND2* (R422*)**	***NCOA3* (Q1276del)**	***CASP9* (L89P)**	***WNT10A* (D217N)**	***PDGFRA* (R914Q)**	***SIX1* (D227E)**	***MTF1* (D63E)**	***KDR/VEGFR2* (Q645E)**	***LRRK1* (L416M)**	***TRIM2* (12941G>A)**
Proband	M, ET, P	+/-	+/-	+/-	+/-	+/-	+/-	+/-	+/-	+/-	+/-
First	ET, P	+/-	+/-	+/-	+/-	+/-	+/-	+/-	+/-	+/-	+/-
First	U	+/+	+/+	+/+	+/+	+/+	+/+	+/+	+/+	+/+	+/+
First	M	+/-	+/-	+/-	+/-	+/-	+/+	+/-	+/-	+/-	+/+
Marry-in	U	+/+	+/+	+/+	+/+	+/+	+/+	+/+	+/+	+/+	+/-
Second	ET	+/-	+/+	+/-	+/-	+/-	+/-	+/-	+/-	+/+	+/-
Second	U	+/+	+/+	+/+	+/+	+/+	+/+	+/+	+/+	+/+	+/+
Second	ET, P	+/+	+/-	+/+	+/+	+/-	+/-	+/+	+/-	+/-	+/-
Marry-in	U	+/+	+/-	+/+	+/+	+/+	+/+	+/+	+/+	+/+	+/+
Third	U	+/+	+/-	+/+	+/+	+/+	+/+	+/+	+/+	+/-	+/+
Third	U	+/+	-/-	+/+	+/+	+/-	+/+	+/+	+/-	+/+	+/+
Third	P	+/+	-/-	+/+	+/+	+/+	+/-	+/+	+/+	+/-	+/-
Second	ET, P	+/-	+/-	+/-	+/-	+/-	+/-	+/-	+/-	+/+	+/+
Second	U	+/+	+/-	+/-	+/-	+/+	+/+	+/-	+/+	+/+	+/-
Second	U	+/-	+/-	+/-	+/-	+/+	+/-	+/-	+/+	+/-	+/-
Second	ET, P	+/+	+/-	+/+	+/+	+/-	+/-	+/-	+/-	+/+	+/-
Second	U	+/-	+/-	+/+	+/+	+/+	+/+	+/-	+/+	+/+	+/-
Marry-in	U	+/+	+/-	+/+	+/+	+/+	+/+	+/+	+/+	+/+	+/-
Marry-in	U	+/+	+/+	+/+	+/+	+/+	+/+	+/+	+/+	+/+	+/+
Third	U	+/+	+/+	+/+	+/-	+/+	+/+	+/+	+/+	+/+	+/+
Third	U	+/-	+/-	+/+	+/-	+/+	+/+	+/-	+/+	+/+	+/+
Marry-in	U	+/+	+/-	+/+	+/+	+/+	+/+	+/+	+/+	+/+	+/+
Third	U	+/+	+/+	+/+	+/+	+/+	+/+	+/+	+/+	+/+	+/+

+/+ indicates homozygous for wild type alleles; +/- indicates heterozygous for the mutation; -/- indicates homozygous for the mutation; M: macrostomia; ET: Ear tag; P: Ptosis; U: unaffected

We used TDT tests to examine associations between each gene and the binarized phenotype 'affected/unaffected', where affected was defined as having any number of OAVS anomalies. Moreover, we used a penalized regression method to analyze the genes together as a system, where the outcome was the burden of OAVS anomalies. The burden outcome was defined as a number on a scale, ranging from 0 (no OAVS phenotypes) to 3 (the proposita, who has all 3 OAVS phenotypes). Of the 23 family members represented in this study, 6 presented uni- or bilateral ptosis, 6 presented ear tags, and 2 presented macrostomia and a total of 5 individuals presented multiple OAVS phenotypes. It is important to mention that there were an additional 5 individuals in the original family who were described as presenting an abnormal mouth phenotype described as an atypical angle of the mouth with the lower lip vermillion shorter than the upper lip and a broad and irregular commissure[1]. For the purposes of these analyses, only the two individuals with the most severe mouth phenotypes (III-1 (macrostomia) and III-5 (wide mouth) were considered as affected with macrostomia.

As seen in Table 5, the results of these sib-TDTs indicate that mutations in genes *PDGFRA* and *KDR/VEGFR2* were associated with the ear tags phenotype. We noted that *PDGFRA* and *KDR/VEGFR2* are in high linkage disequilibrium and thus, all individuals with a mutation in *PDGFRA* also have a mutation in *KDR/VEGFR2*.

Table 5: Results from phenotype specific TDTs

CHR	Gene	A1	A2	P	Phenotype
1	*CASP9*	G	A	0.96	Uni- or bilateral ptosis
1	*MTF1*	A	C	0.89	Uni- or bilateral ptosis
2	*WNT10A*	A	G	0.96	Uni- or bilateral ptosis
4	*PDGFRA*	A	G	0.2	Uni- or bilateral ptosis
4	*KDR/VEGFR2*	G	C	0.2	Uni- or bilateral ptosis
4	*TRIM2*	A	G	0.5	Uni- or bilateral ptosis
7	*KCND2*	T	C	0.96	Uni- or bilateral ptosis
14	***SIX1***	**T**	**C**	**0.05**	**Uni- or bilateral ptosis**
15	*LRRK1*	A	C	0.36	Uni- or bilateral ptosis
1	*CASP9*	G	A	0.58	Ear Tags
1	*MTF1*	A	C	0.63	Ear Tags
2	*WNT10A*	A	G	0.58	Ear Tags
4	***PDGFRA***	**A**	**G**	**<0.01**	**Ear Tags**
4	***KDR/VEGFR2***	**G**	**C**	**<0.01**	**Ear Tags**
4	*TRIM2*	A	G	0.81	Ear Tags
7	*KCND2*	T	C	0.58	Ear Tags
14	***SIX1***	**T**	**C**	**0.01**	**Ear Tags**
15	*LRRK1*	A	C	0.9	Ear Tags
1	*CASP9*	G	A	0.16	Macrostomia

1	*MTF1*	A	C	0.16	Macrostomia
2	*WNT10A*	A	G	0.16	Macrostomia
4	*PDGFRA*	A	G	0.16	Macrostomia
4	*KDR/VEGFR2*	G	C	0.16	Macrostomia
4	*TRIM2*	A	G	0.48	Macrostomia
7	*KCND2*	T	C	0.16	Macrostomia
14	*SIX1*	T	C	0.48	Macrostomia
15	*LRRK1*	A	C	0.16	Macrostomia

Bold indicates significant association with p-values<0.05

The data also show that there is nominal association (P<0.05) between mutations in the *SIX1* gene and the ear tag phenotype. In the tests examining the uni- or bilateral ptosis phenotype, the mutation in *SIX1* had the strongest association compared to other candidate gene mutations. No genetic mutations showed an association with macrostomia at this time. Future analyses including a broader definition of the macrostomia phenotype will be considered to assess the impact of these mutations on the macrostomia spectrum.

Bioinformatic

Following the statistical analysis identifying *SIX1, PDGFRA,* and *KDR/VEGFR2/ VEGFR2* as significantly associated mutations; we investigated the potential functional implications of these mutations.

PDGFRA (platelet derived growth factor receptor alpha) is a cell surface tyrosine kinase receptor. As listed in the InterPro classification, while the mutation site identified in this study is not part of the active site (p.814-p.826), it does come in at the end of the overall kinase domain (p.593-p.954). To further dig into this mutation, we turned to AlphaMissense [51] which trained a two-stage neural network to incorporate predicted 3D structure (similar to AlphaFold) and abundance of known human proteins and calibrated against the ClinVar database of known relationships between protein variants and human health conditions to generate a predicted probability of the input variant being pathogenic. For the p.R914Q mutation, AlphaMissense classifies it as having an 80% probability of pathogenicity (along with a mean 93% probability of all mutations at that site).

Turning to *SIX1*, a transcription factor involved in embryonic development and often co-expressed with *EYA1*, InterPro indicates that p.217 does not occur within the primary homeodomain. However, MobiDB, a *database* of protein disorder and mobility, predicts that p.227 exists within a Linear Interacting Peptide (LIP) region, as well as a 99bp Intrinsically Disordered Region. Such proteins do not attain “stable three-dimensional structure under physiological conditions” and can display a high degree of conformational flexibility that endows proteins or protein regions with functional promiscuity [59]. When we look at the exchange of Aspartic Acid for Glutamic acid in the p.D227E mutation, we see a move to a higher molecular weight residue with a larger van der Waals volume. Combined with the fact that LIP regions are responsible for mediating protein-protein interactions and the mutation further being within an IDR, indicates a role for the mutation to interfere with protein flexibility and potentially the regulatory function.

Finally, *KDR/VEGFR2/* (vascular endothelial growth factor receptor 2) encodes a kinase insert domain receptor of *VEGF*(A/C/D) that is essential for vascular development and hematopoiesis [Uniprot P35968]. InterPro indicates that p.645 occurs within a protein kinase domain (similar to *PDGFRA*) and Q645E is a known missense mutation listed in COSMIC

(Catalogue of Somatic Mutations in Cancer) [COSV55760314] that affects the VEGF signaling, angiogenesis, and focal adhesion pathways.

Moving beyond the implications of individual genes/proteins, we turned to pathway overrepresentation analysis through the R package pathfindR. This method was chosen specifically because pathfindR, prior to performing pathway analysis, filters the input genes through databases of protein-protein interaction networks (PIN) to ensure validated interactions with at most one intervening protein. Using the Biogrid PIN we identified connections between *KDR/VEGFR2* and *PDGFRA* with *CAV1* as an intermediary implicated in GO pathways for peptidyl-tyrosine phosphorylation (GO:0018108), positive regulation of phosphatidylinositol 3-kinase signaling (GO:0014068), and transmembrane receptor protein tyrosine kinase activity (GO:0004714). Furthermore, *SIX1* and *PDGFRA* were connected by FZR1 in the embryonic cranial skeleton morphogenesis (GO:0048701) pathway. Finally, *KDR/VEGFR2* and *PDGFRA* were connected in the Reactome database within the signaling by *PDGFRA* in disease (R-HSA-9671555) pathway, further validating the AlphaMissense results.

Discussion

OAVS is the second most common craniofacial birth defect. Rehabilitation of the wide spectrum of anomalies in individuals with OAVS requires multidisciplinary surgical care throughout life. Its complex etiology remains poorly understood despite the many case reports and several associated genetic and environmental factors. In this study, we present the molecular findings of a family affected with macrostomia or abnormal mouth contour, preauricular tags, and uni- or bilateral uni- or bilateral ptosis. According to the original clinical description of this family, there are no hearing, spine, limbs, or renal defects [1].

The study of large families with incomplete penetrance and wide phenotypic variability allows us to search not only causal genes but also possible modifiers, both genetic and non-genetic. Although our results for this large family indicated that the disease follows an autosomal dominant inheritance; our analysis showed that missense mutations on the genes *SIX1*, *PDGFRA* and *KDR/VEGFR2* had the best evidence of segregation with the OAVS phenotypes in this family.

SIX1 haploinsufficiency or hypomorphic mutations in *SIX* genes have been reported in patients with Branchio-oto-renal syndrome (BOR) (OMIM 113650), renal dysplasia, hearing loss, and frontonasal dysplasia syndrome[60]. BOR has craniofacial and vertebral signs similar to OAVS. Studies of *Six* genes in Drosophila show that the *Six* gene family is essential for eye morphogenesis [61]; and in mice, *Six1* is required for normal development of the kidney, muscle and inner ear, midface and mandibular structures and is co-expressed with Eya factors [33, 62-64]. *EYA* proteins interact with *SIX* proteins during development and the interaction causes *EYA* proteins to translocate to the nucleus and as a complex *SIX-EYA* can activate gene transcription[65]. Interestingly, *EYA1* is also involved in BOR and mutations in *EYA3* have been detected in patients with OAVS [22, 23]. Moreover, a *DACH1* deletion and a *DACH2* duplication were recently described in two independent patients with OAVS[66]. These data support that dysregulation of the Retinal Determination Gene Network (*RDGN*) of genes also known in animals as the *PSEDN (PAX-SIX-EYA-DACH* network) which functions in eye development and others such as muscles, endocrine glands, placodes, and pharyngeal pouches is involved in the etiology of OAVS[67].

In addition to the evidence from previous studies, our *in-silico* analysis for *SIX1* shows that the missense mutation D227E found in this family has the potential to interfere with the protein flexibility and its regulatory function. Lastly, Richieri-Costa pointed out that the external ophthalmoplegia presented by some family members that were affected with uni- or bilateral ptosis should be differentiated[1]. Notably, *Six 1* deficiency in mice causes reduced and disorganized muscle mass [68] and *Six 4* causes exacerbated craniofacial defects and severe

muscle hypoplasia [69]. Finally, a study with adult mice showed that *Six1* and *Eya1* are implicated in the establishment and control of the fast-twitch skeletal muscle phenotype[69].

PDGFRA is Tyrosine-protein kinase that acts as a cell-surface receptor for platelet-derived growth factors *PDGFA, PDGFB* and *PDGFC* with a key role on regulation of embryonic craniofacial and neural crest development, palatogenesis and neural tube closure[70-72]. Mice homozygous but not heterozygous mutants for *Pdgfra* have cleft palate due to NCCS migration defects, however after ethanol exposure both homozygous and heterozygous *Pdgfra* mutans developed profound defects in the palate and pharyngeal skeleton related to neural crest apoptosis and suggesting a protective role against ethanol-induced craniofacial defects [73]. Interestingly, a *PDGFRA* (c.C2740T; p.R914W) rare missense mutation was found to be functional with a dominant negative effect on a family with multiple affected with nonsyndromic OFC exhibiting decreased penetrance. This is in the same amino acid residue from our *PDGFRA* mutation R914Q. The wild-type (R914) forms direct hydrogen bonds with I909, Y913 and W933 plus three additional amino acids (I909, G912 and S935) [74] and it is likely that our mutation R914Q just like R914W obliterates some or all of these hydrogene bonds[75]. Lastly, in zebrafish, genetic alteration of *Pdgfra* caused unilateral clefts of the upper lip[75], which could relate to the macrostomia defect which is also a form of facial cleft in the family presented.

The *KDR/VEGFR2* gene encodes for a Tyrosine-protein kinase that acts as a cell-surface receptor for *VEGFA, VEGFC* and *VEGFD*[76] and mediates VEGF-induced endothelial proliferation, survival, migration, tubular morphogenesis and sprouting. The Vascular Endothelial Growth Factors (*VEGFs*) / receptors (*VEGFRs*) system plays an important role in angiogenesis, as well as osteogenesis, during bone development, growth, and remodeling, attracting endothelial cells and osteoclasts and stimulating osteoblast differentiation. *VEGFR2* mediates differentiation and proliferation of endothelial cells, and it is express in osteoblasts and osteoclasts, particularly during bone remodeling (Byun et al., 2007), Also *VEGFR1, VEGFR2* and VEGFR3 are expressed in both human and fetal and adult bone albeit with significantly higher expression in fetal samples especially in mandibles[77]. The higher expression of *KDR/VEGFR2* on fetal mandibles correlated well with the OAVS condition where microsomia and micrognathia are common occurrences. During mandibular development the neural crest cell-derived VEGF promotes adequate vessel growth and arterial stability and vessel-derived factors enable appropriate levels of chondrocyte proliferation and morphogenesis of Meckel's cartilage, which are essential for mandibular enlargement[78]. The loss of VEGF reduces chondrocyte proliferation in Meckel's cartilage and impairs jaw outgrowth. Cases with hemifacial microsomia also present malformations of the mandibular artery and reduction of mandibular medullary cavity volume that correlates with mandibular hypoplasia[78]. Finally, relevant to reconstructive surgery, *VEGFR2* is mostly produced during the early period of bone regeneration and modulation of *VEGF/VEGFR* could contribute to graft integration and improve outcomes for OAVS cases undergoing surgical reconstruction[79].
Related to ocular phenotypes present in the OAVS condition, both *VEGF* and *KDR/VEGFR2* transcripts have correlated expression during the normal development of the ocular vasculature in humans during early development and in later stages *KDR* is linked to the development of the retinal vascular system[80].

The presence of more than one likely pathogenic mutation in the same family raise different possibilities.(1) it confirms the complex etiology of the disease; (2) it is possible that one of the mutations is the main pathogenic mechanism and the additional mutations are modifiers or contributors to the phenotypic variability assuming the genes act on interacting pathways; (3) the multiple heterozygote mutations may be independent events, each one contributing to a distinct phenotype ("multiple hits") yet their additive effects increases the risk for multiple phenotypes to simultaneously appear on an individual has seen in the craniofacial microsomia family with digenic inheritance due to mutations in *EYA3* and *EFTUD2*[81]. Complex, nontraditional models of inheritance should include incomplete penetrance, environmental and

epigenetic factors. Epigenomic studies can explain how genes and environmental exposures interact to affect craniofacial development and lead to disease phenotype.

The recent advances of whole genome technologies and the ability to integrate different OMICs platforms will likely shed light into the regulatory landscape underlying the OAVS, filling the gaps in genotype-phenotype correlations improving diagnosis patient care and paving the way for future prevention strategies.

Acknowledgments

Funding: Dewel Endowed funds University of Iowa Department of Orthodontics; NIDCR K01DE027995; Iowa Institute for Oral Health Research

References

1. Richieri-Costa A, Ribeiro LA. Macrostomia, preauricular tags, and external ophthalmoplegia: a new autosomal dominant syndrome within the oculoauriculovertebral spectrum? Cleft Palate Craniofac J. 2006;43(4):429-34. doi: 10.1597/05-060.1. PubMed PMID: 16854200.

2. Gorlin RJ, Jue KL, Jacobsen U, Goldschmidt E. OCULOAURICULOVERTEBRAL DYSPLASIA. J Pediatr. 1963;63:991-9. doi: 10.1016/s0022-3476(63)80233-4. PubMed PMID: 14071056.

3. Chen Q, Zhao Y, Shen G, Dai J. Etiology and Pathogenesis of Hemifacial Microsomia. Journal of dental research. 2018;97(12):1297-305. doi: 10.1177/0022034518795609.

4. Kobraei EM, Lentz AK, Eberlin KR, Hachach-Haram N, Hamdan US. Macrostomia: A Practical Guide for Plastic and Reconstructive Surgeons. The Journal of craniofacial surgery. 2016;27(1):118-23. doi: 10.1097/scs.0000000000002294. PubMed PMID: 26703052.

5. Tarle M, Tarle A, Macan D, Knežević Krajina H, Knežević P. Isolated bilateral macrostomia: literature review and case report. Eur J Paediatr Dent. 2023;24(1):56-60. doi: 10.23804/ejpd.2023.24.01.10. PubMed PMID: 36853212.

6. Alhusainan H, Bartlett SP, Gilardino MS. 19 - Rare Craniofacial Clefts. In: Farhadieh RD, Bulstrode NW, Mehrara BJ, Cugno S, editors. Plastic Surgery - Principles and Practice: Elsevier; 2022. p. 248-66.

7. Kawai T, Kurita K, Echiverre NV, Natsume N. Modified technique in surgical correction of macrostomia. International journal of oral and maxillofacial surgery. 1998;27(3):178-80. doi: 10.1016/s0901-5027(98)80005-2. PubMed PMID: 9662008.

8. Askar I, Gurlek A, Sevin K. Lateral facial clefts (macrostomia). Ann Plast Surg. 2001;47(3):355-6. doi: 10.1097/00000637-200109000-00034. PubMed PMID: 11562056.

9. Gunturu S, Nallamothu R, Kodali RM, Nadella KR, Guttikonda LK, Uppaluru V. Macrostomia: a review of evolution of surgical techniques. Case Rep Dent. 2014;2014:471353. Epub 20140929. doi: 10.1155/2014/471353. PubMed PMID: 25400956; PMCID: PMC4220568.

10. Beck AE, Hudgins L, Hoyme HE. Autosomal dominant microtia and ocular coloboma: new syndrome or an extension of the oculo-auriculo-vertebral spectrum? American journal of medical genetics Part A. 2005;134(4):359-62. doi: 10.1002/ajmg.a.30638. PubMed PMID: 15800906.

11. García-Castro M, Martinez-Merino T, Puente N, Riancho JA. Expanding the Etiology of Oculo-Auriculo-Vertebral Spectrum: A Novel Interstitial Microdeletion at 1p36. Int J Mol Sci. 2022;24(1). Epub 20221220. doi: 10.3390/ijms24010036. PubMed PMID: 36613479; PMCID: PMC9820115.

12. Chen Q, Zhao Y, Shen G, Dai J. Etiology and Pathogenesis of Hemifacial Microsomia. Journal of dental research. 2018;97(12):1297-305. Epub 20180911. doi: 10.1177/0022034518795609. PubMed PMID: 30205013.

13. Gougoutas AJ, Singh DJ, Low DW, Bartlett SP. Hemifacial microsomia: clinical features and pictographic representations of the OMENS classification system. Plast Reconstr Surg. 2007;120(7):112e-3e. doi: 10.1097/01.prs.0000287383.35963.5e. PubMed PMID: 18090735.

14. Werler MM, Starr JR, Cloonan YK, Speltz ML. Hemifacial microsomia: from gestation to childhood. The Journal of craniofacial surgery. 2009;20 Suppl 1(Suppl 1):664-9. doi: 10.1097/SCS.0b013e318193d5d5. PubMed PMID: 19218862; PMCID: PMC2791372.

15. Guida V, Calzari L, Fadda MT, Piceci-Sparascio F, Digilio MC, Bernardini L, Brancati F, Mattina T, Melis D, Forzano F, Briuglia S, Mazza T, Bianca S, Valente EM, Salehi LB, Prontera P, Pagnoni M, Tenconi R, Dallapiccola B, Iannetti G, Corsaro L, De Luca A, Gentilini D. Genome-Wide DNA Methylation Analysis of a Cohort of 41 Patients Affected by Oculo-Auriculo-Vertebral Spectrum (OAVS). Int J Mol Sci. 2021;22(3). Epub 20210126. doi: 10.3390/ijms22031190. PubMed PMID: 33530447; PMCID: PMC7866060.

16. Lopez E, Berenguer M, Tingaud-Sequeira A, Marlin S, Toutain A, Denoyelle F, Picard A, Charron S, Mathieu G, de Belvalet H, Arveiler B, Babin PJ, Lacombe D, Rooryck C. Mutations in MYT1, encoding the myelin transcription factor 1, are a rare cause of OAVS. Journal of medical genetics. 2016;53(11):752-60. Epub 20160629. doi: 10.1136/jmedgenet-2016-103774. PubMed PMID: 27358179.

17. Berenguer M, Tingaud-Sequeira A, Colovati M, Melaragno MI, Bragagnolo S, Perez ABA, Arveiler B, Lacombe D, Rooryck C. A novel de novo mutation in MYT1, the unique OAVS gene identified so far. European journal of human genetics : EJHG. 2017;25(9):1083-6. Epub 20170614. doi: 10.1038/ejhg.2017.101. PubMed PMID: 28612832; PMCID: PMC5558169.

18. Luquetti DV, Heike CL, Zarante I, Timms AE, Gustafson J, Pachajoa H, Porras-Hurtado GL, Ayala-Ramirez P, Duenas-Roque MM, Jimenez N, Ibanez LM, Hurtado-Villa P. MYT1 role in the microtia-craniofacial microsomia spectrum. Molecular genetics & genomic medicine. 2020;8(10):e1401. Epub 20200901. doi: 10.1002/mgg3.1401. PubMed PMID: 32871052; PMCID: PMC7549594.

19. Zamariolli M, Burssed B, Moysés-Oliveira M, Colovati M, Bellucco FTdS, dos Santos LC, Alvarez Perez AB, Bragagnolo S, Melaragno MI. Novel MYT1 variants expose the complexity of oculo-auriculo-vertebral spectrum genetic mechanisms. American Journal of Medical Genetics Part A. 2021;185(7):2056-64. doi: https://doi.org/10.1002/ajmg.a.62217.

20. Timberlake AT, Griffin C, Heike CL, Hing AV, Cunningham ML, Chitayat D, Davis MR, Doust SJ, Drake AF, Duenas-Roque MM, Goldblatt J, Gustafson JA, Hurtado-Villa P, Johns A, Karp N, Laing NG, Magee L, Mullegama SV, Pachajoa H, Porras-Hurtado GL, Schnur RE, Slee J, Singer SL, Staffenberg DA, Timms AE, Wise CA, Zarante I, Saint-Jeannet J-P, Luquetti DV, University of Washington Center for Mendelian G. Haploinsufficiency of SF3B2 causes craniofacial microsomia. Nature Communications. 2021;12(1):4680. doi: 10.1038/s41467-021-24852-9.

21. Tingaud-Sequeira A, Trimouille A, Marlin S, Lopez E, Berenguer M, Gherbi S, Arveiler B, Lacombe D, Rooryck C. Functional and genetic analyses of ZYG11B provide evidences for its involvement in OAVS. Molecular genetics & genomic medicine. 2020;8(10):e1375. Epub 20200801. doi: 10.1002/mgg3.1375. PubMed PMID: 32738032; PMCID: PMC7549578.

22. Tingaud-Sequeira A, Trimouille A, Salaria M, Stapleton R, Claverol S, Plaisant C, Bonneu M, Lopez E, Arveiler B, Lacombe D, Rooryck C. A recurrent missense variant in EYA3 gene is associated with oculo-auriculo-vertebral spectrum. Hum Genet. 2021;140(6):933-44. Epub 20210121. doi: 10.1007/s00439-021-02255-6. PubMed PMID: 33475861.

23. Si N, Zhan G, Meng X, Zhang Z, Huang X, Pan B. Identification of novel mutations in EYA3 and EFTUD2 in a family with craniofacial microsomia: evidence of digenic inheritance. Front Med. 2023;17(5):1006-9. Epub 20230729. doi: 10.1007/s11684-023-1000-3. PubMed PMID: 37507637.

24. Wang Y, Ping L, Luan X, Chen Y, Fan X, Li L, Liu Y, Wang P, Zhang S, Zhang B, Chen X. A Mutation in VWA1, Encoding von Willebrand Factor A Domain-Containing Protein 1, Is

Associated With Hemifacial Microsomia. Front Cell Dev Biol. 2020;8:571004. Epub 20200909. doi: 10.3389/fcell.2020.571004. PubMed PMID: 33015062; PMCID: PMC7509151.

25. Trimouille A, Tingaud-Sequeira A, Lacombe D, Duelund Hjortshøj T, Kreiborg S, Buciek Hove H, Rooryck C. Description of a family with X-linked oculo-auriculo-vertebral spectrum associated with polyalanine tract expansion in ZIC3. Clinical genetics. 2020;98(4):384-9. doi: 10.1111/cge.13811. PubMed PMID: 32639022.

26. Rengasamy Venugopalan S, Farrow E, Sanchez-Lara PA, Yen S, Lypka M, Jiang S, Allareddy V. A novel nonsense substitution identified in the AMIGO2 gene in an Occulo-Auriculo-Vertebral spectrum patient. Orthod Craniofac Res. 2019;22 Suppl 1:163-7. doi: 10.1111/ocr.12259. PubMed PMID: 31074142.

27. Zamariolli M, Colovati M, Moysés-Oliveira M, Nunes N, Caires Dos Santos L, Alvarez Perez AB, Bragagnolo S, Melaragno MI. Rare single-nucleotide variants in oculo-auriculo-vertebral spectrum (OAVS). Molecular genetics & genomic medicine. 2019;7(10):e00959. Epub 20190830. doi: 10.1002/mgg3.959. PubMed PMID: 31469246; PMCID: PMC6785430.

28. Fan Z, Du J, Liu H, Zhang H, Dlugosz AA, Wang CY, Fan M, Shen Y, Wang S. A susceptibility locus on 1p32-1p34 for congenital macrostomia in a Chinese family and identification of a novel PTCH2 mutation. American journal of medical genetics Part A. 2009;149a(3):521-4. doi: 10.1002/ajmg.a.32647. PubMed PMID: 19208383.

29. Rooryck C, Souakri N, Cailley D, Bouron J, Goizet C, Delrue MA, Marlin S, Lacombe FD, Arveiler B. Array-CGH analysis of a cohort of 86 patients with oculoauriculovertebral spectrum. American journal of medical genetics Part A. 2010;152a(8):1984-9. doi: 10.1002/ajmg.a.33491. PubMed PMID: 20635336.

30. Ballesta-Martínez MJ, López-González V, Dulcet LA, Rodríguez-Santiago B, Garcia-Miñaúr S, Guillen-Navarro E. Autosomal dominant oculoauriculovertebral spectrum and 14q23.1 microduplication. American journal of medical genetics Part A. 2013;161a(8):2030-5. Epub 20130621. doi: 10.1002/ajmg.a.36007. PubMed PMID: 23794319.

31. Bragagnolo S, Colovati MES, Souza MZ, Dantas AG, F de Soares MF, Melaragno MI, Perez AB. Clinical and cytogenomic findings in OAV spectrum. American Journal of Medical Genetics Part A. 2018;176(3):638-48. doi: https://doi.org/10.1002/ajmg.a.38576.

32. Northup JK, Matalon D, Hawkins JC, Matalon R, Velagaleti GVN. Pericentric inversion, inv(14)(p11.2q22.3), in a 9-month old with features of Goldenhar syndrome. Clin Dysmorphol. 2010;19(4):185-9. doi: 10.1097/MCD.0b013e3283359386. PubMed PMID: 20571379.

33. Ou Z, Martin DM, Bedoyan JK, Cooper ML, Chinault AC, Stankiewicz P, Cheung SW. Branchiootorenal syndrome and oculoauriculovertebral spectrum features associated with duplication of SIX1, SIX6, and OTX2 resulting from a complex chromosomal rearrangement. American Journal of Medical Genetics Part A. 2008;146A(19):2480-9. doi: https://doi.org/10.1002/ajmg.a.32398.

34. Si N, Meng X, Lu X, Liu Z, Qi Z, Wang L, Li C, Yang M, Zhang Y, Wang C, Guo P, Zhu L, Liu L, Li Z, Zhang Z, Cai Z, Pan B, Jiang H, Zhang X. Duplications involving the long range HMX1 enhancer are associated with human isolated bilateral concha-type microtia. J Transl Med. 2020;18(1):244. doi: 10.1186/s12967-020-02409-6.

35. Si N, Zhang Z, Meng X, Huang X, Wang C, Pan B. Generation of an induced pluripotent stem cell line from a congenital microtia patient with 4p16.1 microduplication involving the long-range enhancer of HMX1. Stem Cell Res. 2021;53:102357. Epub 20210421. doi: 10.1016/j.scr.2021.102357. PubMed PMID: 34087987.

36. Spineli-Silva S, Sgardioli IC, Dos Santos AP, Bergamini LL, Monlleó IL, Fontes MIB, Félix TM, Ribeiro EM, Xavier AC, Lustosa-Mendes E, Gil-da-Silva-Lopes VL, Vieira TP. Genomic imbalances in craniofacial microsomia. American journal of medical genetics Part C, Seminars in medical genetics. 2020;184(4):970-85. Epub 20201120. doi: 10.1002/ajmg.c.31857. PubMed PMID: 33215817.

37. Tingaud-Sequeira A, Trimouille A, Sagardoy T, Lacombe D, Rooryck C. Oculo-auriculo-vertebral spectrum: new genes and literature review on a complex disease. Journal of medical genetics. 2022;59(5):417-27. Epub 20220202. doi: 10.1136/jmedgenet-2021-108219. PubMed PMID: 35110414.

38. Zielinski D, Markus B, Sheikh M, Gymrek M, Chu C, Zaks M, Srinivasan B, Hoffman JD, Aizenbud D, Erlich Y. OTX2 Duplication Is Implicated in Hemifacial Microsomia. PLoS One. 2014;9(5):e96788. doi: 10.1371/journal.pone.0096788.

39. Vendramini-Pittoli S, Kokitsu-Nakata NM. Oculoauriculovertebral spectrum: report of nine familial cases with evidence of autosomal dominant inheritance and review of the literature. Clin Dysmorphol. 2009;18(2):67-77. doi: 10.1097/MCD.0b013e328323a7dd. PubMed PMID: 19305190.

40. Celse T, Tingaud-Sequeira A, Dieterich K, Siegfried G, Lecaignec C, Bouneau L, Fannemel M, Salaun G, Laffargue F, Martinez G, Satre V, Vieville G, Bidart M, Soussi Zander C, Turesson AC, Splitt M, Reboul D, Chiesa J, Khau Van Kien P, Godin M, Gruchy N, Goel H, Palmer E, Demetriou K, Shalhoub C, Rooryck C, Coutton C. OTX2 duplications: a recurrent cause of oculo-auriculo-vertebral spectrum. Journal of medical genetics. 2023;60(6):620-6. Epub 20221111. doi: 10.1136/jmg-2022-108678. PubMed PMID: 36368868.

41. Tasse C, Majewski F, Böhringer S, Fischer S, Lüdecke HJ, Gillessen-Kaesbach G, Wieczorek D. A family with autosomal dominant oculo-auriculo-vertebral spectrum. Clin Dysmorphol. 2007;16(1):1-7. doi: 10.1097/MCD.0b013e328010d313. PubMed PMID: 17159507.

42. Betschart RO, Thiéry A, Aguilera-Garcia D, Zoche M, Moch H, Twerenbold R, Zeller T, Blankenberg S, Ziegler A. Comparison of calling pipelines for whole genome sequencing: an empirical study demonstrating the importance of mapping and alignment. Sci Rep. 2022;12(1):21502. Epub 20221213. doi: 10.1038/s41598-022-26181-3. PubMed PMID: 36513709; PMCID: PMC9748128.

43. Zhao S, Agafonov O, Azab A, Stokowy T, Hovig E. Accuracy and efficiency of germline variant calling pipelines for human genome data. Sci Rep. 2020;10(1):20222. Epub 20201119. doi: 10.1038/s41598-020-77218-4. PubMed PMID: 33214604; PMCID: PMC7678823.

44. Adzhubei I, Jordan DM, Sunyaev SR. Predicting functional effect of human missense mutations using PolyPhen-2. Curr Protoc Hum Genet. 2013;Chapter 7:Unit7.20. doi: 10.1002/0471142905.hg0720s76. PubMed PMID: 23315928; PMCID: PMC4480630.

45. Kircher M, Witten DM, Jain P, O'Roak BJ, Cooper GM, Shendure J. A general framework for estimating the relative pathogenicity of human genetic variants. Nat Genet. 2014;46(3):310-5. doi: 10.1038/ng.2892.

46. Kopanos C, Tsiolkas V, Kouris A, Chapple CE, Albarca Aguilera M, Meyer R, Massouras A. VarSome: the human genomic variant search engine. Bioinformatics. 2019;35(11):1978-80. doi: 10.1093/bioinformatics/bty897. PubMed PMID: 30376034; PMCID: PMC6546127.

47. Ewens WJ, Spielman RS. The transmission/disequilibrium test: history, subdivision, and admixture. Am J Hum Genet. 1995;57(2):455-64. PubMed PMID: 7668272; PMCID: PMC1801556.

48. Spielman RS, Ewens WJ. A sibship test for linkage in the presence of association: the sib transmission/disequilibrium test. Am J Hum Genet. 1998;62(2):450-8. doi: 10.1086/301714. PubMed PMID: 9463321; PMCID: PMC1376890.

49. Reisetter AC, Breheny P. Penalized linear mixed models for structured genetic data. Genetic epidemiology. 2021;45(5):427-44. Epub 20210516. doi: 10.1002/gepi.22384. PubMed PMID: 33998038.

50. Paysan-Lafosse T, Blum M, Chuguransky S, Grego T, Pinto BL, Salazar Gustavo A, Bileschi Maxwell L, Bork P, Bridge A, Colwell L, Gough J, Haft Daniel H, Letunić I, Marchler-Bauer A, Mi H, Natale Darren A, Orengo Christine A, Pandurangan Arun P, Rivoire C, Sigrist CJA, Sillitoe I, Thanki N, Thomas PD, Tosatto SCE, Wu Cathy H, Bateman A. InterPro in 2022. Nucleic acids research. 2023;51(D1):D418-D27. doi: 10.1093/nar/gkac993.

51. Cheng J, Novati G, Pan J, Bycroft C, Žemgulytė A, Applebaum T, Pritzel A, Wong LH, Zielinski M, Sargeant T, Schneider RG, Senior AW, Jumper J, Hassabis D, Kohli P, Avsec Ž. Accurate proteome-wide missense variant effect prediction with AlphaMissense. Science.381(6664):eadg7492. doi: 10.1126/science.adg7492.

52. Piovesan D, Del Conte A, Clementel D, Monzon Alexander M, Bevilacqua M, Aspromonte Maria C, Iserte Javier A, Orti FE, Marino-Buslje C, Tosatto Silvio CE. MobiDB: 10 years of intrinsically disordered proteins. Nucleic acids research. 2023;51(D1):D438-D44. doi: 10.1093/nar/gkac1065.

53. Ulgen E, Ozisik O, Sezerman OU. pathfindR: An R Package for Comprehensive Identification of Enriched Pathways in Omics Data Through Active Subnetworks. Frontiers in Genetics. 2019;10. doi: 10.3389/fgene.2019.00858.

54. Chatr-aryamontri A, Oughtred R, Boucher L, Rust J, Chang C, Kolas NK, O'Donnell L, Oster S, Theesfeld C, Sellam A, Stark C, Breitkreutz B-J, Dolinski K, Tyers M. The BioGRID interaction database: 2017 update. Nucleic acids research. 2017;45(D1):D369-D79. doi: 10.1093/nar/gkw1102.

55. Stark C, Breitkreutz B-J, Reguly T, Boucher L, Breitkreutz A, Tyers M. BioGRID: a general repository for interaction datasets. Nucleic acids research. 2006;34(suppl_1):D535-D9. doi: 10.1093/nar/gkj109.

56. Ashburner M, Ball CA, Blake JA, Botstein D, Butler H, Cherry JM, Davis AP, Dolinski K, Dwight SS, Eppig JT, Harris MA, Hill DP, Issel-Tarver L, Kasarskis A, Lewis S, Matese JC, Richardson JE, Ringwald M, Rubin GM, Sherlock G. Gene Ontology: tool for the unification of biology. Nat Genet. 2000;25(1):25-9. doi: 10.1038/75556.

57. Fabregat A, Jupe S, Matthews L, Sidiropoulos K, Gillespie M, Garapati P, Haw R, Jassal B, Korninger F, May B, Milacic M, Roca CD, Rothfels K, Sevilla C, Shamovsky V, Shorser S, Varusai T, Viteri G, Weiser J, Wu G, Stein L, Hermjakob H, D'Eustachio P. The Reactome Pathway Knowledgebase. Nucleic acids research. 2018;46(D1):D649-D55. doi: 10.1093/nar/gkx1132.

58. Karczewski KJ, Francioli LC, Tiao G, Cummings BB, Alföldi J, Wang Q, Collins RL, Laricchia KM, Ganna A, Birnbaum DP, Gauthier LD, Brand H, Solomonson M, Watts NA, Rhodes D, Singer-Berk M, England EM, Seaby EG, Kosmicki JA, Walters RK, Tashman K, Farjoun Y, Banks E, Poterba T, Wang A, Seed C, Whiffin N, Chong JX, Samocha KE, Pierce-Hoffman E, Zappala Z, O'Donnell-Luria AH, Minikel EV, Weisburd B, Lek M, Ware JS, Vittal C, Armean IM, Bergelson L, Cibulskis K, Connolly KM, Covarrubias M, Donnelly S, Ferriera S, Gabriel S, Gentry J, Gupta N, Jeandet T, Kaplan D, Llanwarne C, Munshi R, Novod S, Petrillo N, Roazen D, Ruano-Rubio V, Saltzman A, Schleicher M, Soto J, Tibbetts K, Tolonen C, Wade

G, Talkowski ME, Aguilar Salinas CA, Ahmad T, Albert CM, Ardissino D, Atzmon G, Barnard J, Beaugerie L, Benjamin EJ, Boehnke M, Bonnycastle LL, Bottinger EP, Bowden DW, Bown MJ, Chambers JC, Chan JC, Chasman D, Cho J, Chung MK, Cohen B, Correa A, Dabelea D, Daly MJ, Darbar D, Duggirala R, Dupuis J, Ellinor PT, Elosua R, Erdmann J, Esko T, Färkkilä M, Florez J, Franke A, Getz G, Glaser B, Glatt SJ, Goldstein D, Gonzalez C, Groop L, Haiman C, Hanis C, Harms M, Hiltunen M, Holi MM, Hultman CM, Kallela M, Kaprio J, Kathiresan S, Kim B-J, Kim YJ, Kirov G, Kooner J, Koskinen S, Krumholz HM, Kugathasan S, Kwak SH, Laakso M, Lehtimäki T, Loos RJF, Lubitz SA, Ma RCW, MacArthur DG, Marrugat J, Mattila KM, McCarroll S, McCarthy MI, McGovern D, McPherson R, Meigs JB, Melander O, Metspalu A, Neale BM, Nilsson PM, O'Donovan MC, Ongur D, Orozco L, Owen MJ, Palmer CNA, Palotie A, Park KS, Pato C, Pulver AE, Rahman N, Remes AM, Rioux JD, Ripatti S, Roden DM, Saleheen D, Salomaa V, Samani NJ, Scharf J, Schunkert H, Shoemaker MB, Sklar P, Soininen H, Sokol H, Spector T, Sullivan PF, Suvisaari J, Tai ES, Teo YY, Tiinamaija T, Tsuang M, Turner D, Tusie-Luna T, Vartiainen E, Vawter MP, Ware JS, Watkins H, Weersma RK, Wessman M, Wilson JG, Xavier RJ, Neale BM, Daly MJ, MacArthur DG, Genome Aggregation Database C. The mutational constraint spectrum quantified from variation in 141,456 humans. Nature. 2020;581(7809):434-43. doi: 10.1038/s41586-020-2308-7.

59. Trivedi R, Nagarajaram HA. Intrinsically Disordered Proteins: An Overview. Int J Mol Sci [Internet]. 2022; 23 22. Available from: https://mdpi-res.com/d_attachment/ijms/ijms-23-14050/article_deploy/ijms-23-14050-v3.pdf?version=1669097511.

60. Meurer L, Ferdman L, Belcher B, Camarata T. The SIX Family of Transcription Factors: Common Themes Integrating Developmental and Cancer Biology. Frontiers in Cell and Developmental Biology. 2021;9. doi: 10.3389/fcell.2021.707854.

61. Cheyette BN, Green PJ, Martin K, Garren H, Hartenstein V, Zipursky SL. The Drosophila sine oculis locus encodes a homeodomain-containing protein required for the development of the entire visual system. Neuron. 1994;12(5):977-96. doi: 10.1016/0896-6273(94)90308-5. PubMed PMID: 7910468.

62. Tavares ALP, Cox TC, Maxson RM, Ford HL, Clouthier DE. Negative regulation of endothelin signaling by SIX1 is required for proper maxillary development. Development. 2017;144(11):2021-31. Epub 20170428. doi: 10.1242/dev.145144. PubMed PMID: 28455376; PMCID: PMC5482985.

63. Guo C, Sun Y, Zhou B, Adam RM, Li X, Pu WT, Morrow BE, Moon A, Li X. A Tbx1-Six1/Eya1-Fgf8 genetic pathway controls mammalian cardiovascular and craniofacial morphogenesis. J Clin Invest. 2011;121(4):1585-95. doi: 10.1172/jci44630. PubMed PMID: 21364285; PMCID: PMC3069777.

64. Ozaki H, Nakamura K, Funahashi J, Ikeda K, Yamada G, Tokano H, Okamura HO, Kitamura K, Muto S, Kotaki H, Sudo K, Horai R, Iwakura Y, Kawakami K. Six1 controls patterning of the mouse otic vesicle. Development. 2004;131(3):551-62. Epub 20031224. doi: 10.1242/dev.00943. PubMed PMID: 14695375.

65. Soni UK, Roychoudhury K, Hegde RS. The Eyes Absent proteins in development and in developmental disorders. Biochem Soc Trans. 2021;49(3):1397-408. doi: 10.1042/BST20201302.

66. Guida V, Sparascio FP, Bernardini L, Pancheri F, Melis D, Cocciadiferro D, Pagnoni M, Puzzo M, Goldoni M, Barone C, Hozhabri H, Putotto C, Giuffrida MG, Briuglia S, Palumbo O, Bianca S, Stanzial F, Benedicenti F, Kariminejad A, Forzano F, Baghernajad Salehi L, Mattina T, Brancati F, Castori M, Carella M, Fadda MT, Iannetti G, Dallapiccola B, Digilio MC, Marino B, Tartaglia M, De Luca A. Copy number variation analysis implicates novel pathways in patients

with oculo-auriculo-vertebral-spectrum and congenital heart defects. Clin Genet. 2021;100(3):268-79. doi: https://doi.org/10.1111/cge.13994.

67. Kozmik Z, Holland ND, Kreslova J, Oliveri D, Schubert M, Jonasova K, Holland LZ, Pestarino M, Benes V, Candiani S. Pax–Six–Eya–Dach network during amphioxus development: Conservation in vitro but context specificity in vivo. Developmental Biology. 2007;306(1):143-59. doi: https://doi.org/10.1016/j.ydbio.2007.03.009.

68. Laclef C, Hamard G, Demignon J, Souil E, Houbron C, Maire P. Altered myogenesis in Six1-deficient mice. Development. 2003;130(10):2239-52. doi: 10.1242/dev.00440. PubMed PMID: 12668636.

69. Grifone R, Laclef C, Spitz F, Lopez S, Demignon J, Guidotti JE, Kawakami K, Xu PX, Kelly R, Petrof BJ, Daegelen D, Concordet JP, Maire P. Six1 and Eya1 expression can reprogram adult muscle from the slow-twitch phenotype into the fast-twitch phenotype. Mol Cell Biol. 2004;24(14):6253-67. doi: 10.1128/mcb.24.14.6253-6267.2004. PubMed PMID: 15226428; PMCID: PMC434262.

70. Qian C, Wong CWY, Wu Z, He Q, Xia H, Tam PKH, Wong KKY, Lui VCH. Stage specific requirement of platelet-derived growth factor receptor-α in embryonic development. PLoS One. 2017;12(9):e0184473. doi: 10.1371/journal.pone.0184473.

71. Tallquist MD, Soriano P. Cell autonomous requirement for PDGFRalpha in populations of cranial and cardiac neural crest cells. Development. 2003;130(3):507-18. doi: 10.1242/dev.00241. PubMed PMID: 12490557.

72. Joosten PHLJ, Toepoel M, Mariman ECM, Van Zoelen EJJ. Promoter haplotype combinations of the platelet-derived growth factor α-receptor gene predispose to human neural tube defects. Nat Genet. 2001;27(2):215-7. doi: 10.1038/84867.

73. McCarthy N, Wetherill L, Lovely CB, Swartz ME, Foroud TM, Eberhart JK. Pdgfra protects against ethanol-induced craniofacial defects in a zebrafish model of FASD. Development. 2013;140(15):3254-65. doi: 10.1242/dev.094938.

74. Liang L, Yan XE, Yin Y, Yun CH. Structural and biochemical studies of the PDGFRA kinase domain. Biochem Biophys Res Commun. 2016;477(4):667-72. Epub 20160624. doi: 10.1016/j.bbrc.2016.06.117. PubMed PMID: 27349873.

75. Yu Y, Alvarado R, Petty LE, Bohlender RJ, Shaw DM, Below JE, Bejar N, Ruiz OE, Tandon B, Eisenhoffer GT, Kiss DL, Huff CD, Letra A, Hecht JT. Polygenic risk impacts PDGFRA mutation penetrance in non-syndromic cleft lip and palate. Human molecular genetics. 2022;31(14):2348-57. doi: 10.1093/hmg/ddac037.

76. Otrock ZK, Makarem JA, Shamseddine AI. Vascular endothelial growth factor family of ligands and receptors: Review. Blood Cells Mol Dis. 2007;38(3):258-68. doi: https://doi.org/10.1016/j.bcmd.2006.12.003.

77. Marini M, Sarchielli E, Toce M, Acocella A, Bertolai R, Ciulli C, Orlando C, Sgambati E, Vannelli GB. Expression and localization of VEGF receptors in human fetal skeletal tissues. Histol Histopathol. 2012;27(12):1579-87. doi: 10.14670/hh-27.1579. PubMed PMID: 23059888.

78. Wiszniak S, Mackenzie FE, Anderson P, Kabbara S, Ruhrberg C, Schwarz Q. Neural crest cell-derived VEGF promotes embryonic jaw extension. Proceedings of the National Academy of Sciences. 2015;112(19):6086-91. doi: 10.1073/pnas.1419368112.

79. Marini M, Bertolai R, Manetti M, Sgambati E. A case of mandible hypoplasia treated with autologous bone graft from mandibular symphysis: Expression of VEGF and receptors in bone

regeneration. Acta Histochem. 2016;118(6):652-6. doi: https://doi.org/10.1016/j.acthis.2016.07.002.

80. Gogat Kn, Le Gat L, Van Den Berghe Lc, Marchant D, Kobetz A, Gadin Sp, Gasser B, Quéré I, Abitbol M, Menasche M. VEGF and KDR Gene Expression during Human Embryonic and Fetal Eye Development. Invest Ophthalmol Vis Sci. 2004;45(1):7-14. doi: 10.1167/iovs.02-1096.

81. Si N, Zhan G, Meng X, Zhang Z, Huang X, Pan B. Identification of novel mutations in EYA3 and EFTUD2 in a family with craniofacial microsomia: evidence of digenic inheritance. Front Med. 2023;17(5):1006-9. doi: 10.1007/s11684-023-1000-3.

Supplemental Table 1: Genes with LOF and Missense mutations present in the parent and proband but not present in the unaffected grandparent

Missense Mutations	*TTC34, TNFRSF9, H6PD, CASZ1, CASP9, TMEM82, NBPF1, TAS1R2, KDF1, PHACTR4, HCRTR1, MTF1, MACF1, EXO5, FGGY, GNAT2, RAP1A, AP4B1/DCLRE1B, TRIM45, GDAP2, WARS2, NBPF8, KPRP, IVL, SLC27A3, DCST1, RXFP4, RAB25, BCAN, ARHGEF11, OR10J1, MAEL, F5, MR1, GLUL, ASCL5, LAX1, FAM166C, ALK, ELMOD3, CNGA3, POTEI, POTEJ, SCN9A, FSIP2, MFSD6, CD28, UNC80, WNT10A, RETREG2, GIGYF2, UGT1A8/UGT1A10, RAB17, COPS9, CNTN3, FRG2C, ZNF717(5), LNP1, BOC, NPHP3, ZBTB38, FAM131A, MAGEF1, CRMP1, MAN2B2, ACOX3, NIPAL1, PDGFRA, KDR/VEGFR2, PKD2, CCSER1, ZGRF1, TRIM2, C5orf22, LOC105378979, ACTBL2(2), OTP, CAST/ERAP1, PAM, FER, PCDHB16, ATXN1, DCDC2/KAAG1(2), SLC17A4, TNXB, SLC39A7, FGD2, CEP162, RNF146, EPB41L2, TAAR6, TAAR5, TCF21, SMIM28, SYNE1, CNKSR3, LPA, HGC6.3, SDK1, RAPGEF5, BBS9, STEAP2, OR2AE1, PILRB(3), ZAN, MUC3A(5), MUC17, CADPS2, CPA5, TPK1, ACTR3C, ZNF705G, MAFA, PLEC, ANKRD18B, HRCT1, SPAAR, CNTNAP3B(2), CCDC187, AGAP6, GFRA1, KRTAP5-1, KRTAP5-4(2), MUC19(3), MGAT4C, PABPC3(7), POTEM, LMLN2(2), KIAA0586, SIX1, RAD51B, CCDC177, ACOT2, VRTN, ANGEL1, IFI27, TRAF3, ADSS1, PLA2G4D, GANC(2), STARD9(2), UBR1(2), DUOX2, FAM81A, SNX1, C15orf39, CSPG4, ADAMTS7, CTSH, GOLGA6L10(3), GOLGA6L9, SEMA4B, LRRK1, WDR90, PERCC1, NAA60, NDE1, MYH11/NDE1, ABCC1, TK2, ZFP1, BCO1, RNF166, SCGB1C2, KDM6B, FOXO3B, PRPSAP2, KCNJ18(4), CCL3L3, KRTAP2-2, KRTAP4-3, BIRC5, GCGR, TXNDC2(2), SAMD1, C19orf33/YIF1B, ZNF888(2), LENG9, NKX2-2, BPIFB4, CPNE1, TGM2, NCOA3, PELATON, CTSZ, SON, KRTAP10-6/TSPEAR, FAM118A, GAGE12J*
LoF Mutations	*FMO2, KLHDC8A, IFIH1, ATP13A5, PTTG2/TBC1D1, AFP, HGC6.3(2), ZAN, KCND2, PABPC3, GOLGA6D, LOC100128108, PKD1L3*

Numbers in brackets represent the number of mutations found in a gene when more than one mutation was found.